Skin Cancer Detection Using Convolutional Neural Networks

Pedro Silva (n.º 64926)
Pedro Diz (n.º 64852)
Deep Learning, FCUL

Abstract

For the milestone 2 of the project, we present an upgrade over the minimal deep-learning pipeline for binary melanoma detection developed in milestone 1 relative to the ISIC 2018 Task 3 dataset of 11 720 dermoscopic images. After patient-wise splitting (70/15/15), images are cropped, resized, normalized, and augmented before fine-tuning an EfficientNet-B0. With these upgrades and experiments, we can confidently conclude that overall performance improved, the AUROC rose by 2–3 points over the previous baseline.

Keywords: deep learning, dermoscopy, melanoma, skin cancer, EfficientNet, focal loss

1. Introduction

Portugal has a hot climate and extensive beach culture, leading to high sun exposure, which significantly increases the risk of skin cancer[1]. Early detection is crucial, as it greatly improves the chances of successful treatment while reducing long-term damage and increasing survival rates[2]. We propose a solution for detecting cancerous cells using a convolutional neural network. Our approach relies exclusively on the ISIC 2018 Archive. The pipeline includes data acquisition through the ISIC API, preprocessing, model training, and performance evaluation. The source code is available at https://github.com/PedroDiz/AP-2025. This release corresponds to the Baseline 2 version, which achieved the best results.

2. Problem Statement

We address the task of binary classification of dermoscopy skin-lesion images into benign (0) versus malignant (1). Our dataset consists of 11 720 RGB images of size 600×450 pixels drawn from the ISIC 2018 Task 3 challenge.We ignored the challenge's original splits and instead perform a patient-wise stratified split into 70 % training, 15 % validation, and 15 % test. The resulting class distribution is highly imbalanced (figure 1): 81.37 % benign and 18.63 % malignant.

At inference time, the model takes a 600×450 image as input and outputs a malignancy probability $p \in [0, 1]$. Initially, we naively binarize this probability at 0.5, and later evaluate using the Youden point to find the optimal threshold.

We evaluate performance **primarily** using the **AUROC**, which is the standard benchmark metric in dermoscopy and is widely used in related research. **Secondarily**, we report **balanced accuracy** to account for class imbalance. Additional evaluation strategies include the **F_1-score** and **recall**.

3. Technical Approach

3.1. Data Pipeline

We downloaded all images from the ISIC 2018 Task 3 API, split them into multiple ZIP files, and stored them in our repository. In future runs, these ZIP files are downloaded and extracted into a single folder. We then create a single metadata file (`lesions.csv`) containing three columns: image filename, patient ID, and binary label (0=benign, 1=malignant). We performed a patient-wise split into 70 % training, 15 % validation, and 15 % test sets.

Prior to training, each image undergoes the following preprocessing steps:
1. Center-crop to square and resize to 224×224 pixels.
2. Convert to tensor and normalize per-image to zero mean and unit variance.
3. On-the-fly data augmentations *during training only*: random resized crop (scale 0.9–1.0), horizontal and vertical flips, rotation $\pm15°$, color jitter (brightness/contrast/saturation 0.1), and random zoom.

We acknowledge that 5-fold patient-level cross-validation would improve reliability. Our current split depends on a single partition, which may bias results, miss variance, or suffer from unbalanced/easy-hard case distribu-

---

tions. Limited compute prevented this in the current study. Consequently, we retained the original 70%/15%/15% (train/validation/test) split pipeline established in Milestone 1.

3.2. Model Architecture and Training Setup

For the second baseline, we used a CNN backbone from the `timm` library, **EfficientNet-B0**, as we did on the milestone 1, pretrained on ImageNet. The raw model outputs logits z, which are converted to probabilities $p = \sigma(z)$ via a sigmoid activation. Exclusively for this baseline, we added:

- **Mixed-precision + grad-acc:** halves memory usage and doubles effective batch size.
- **Balanced sampler (60/40):** equalizes class exposure per batch (60% benign, 40% malignant), improving minority-class learning.
- **Warm-up freeze:** trains only the new head initially for stable fine-tuning of the pretrained backbone.

All other settings remain as in Milestone 1 (which used a highly imbalanced dataset), but we've reduced the focal BCE *alpha* from 0.75 to 0.6 because we now apply weighted random sampling to up-sample the minority class.

- **Loss function**: We use Focal Binary Cross-Entropy, that up-weights the malignant class relative to the benign class. It extends standard BCE by:
  - α: a class-weight scalar (set to 0.6)
  - γ: the focusing parameter (set to 2)
- **Optimizer**: AdamW with learning rate 3×10^{-4} and weight decay 1×10^{-4}.
- **Scheduler**: Cosine annealing over 30 total epochs.
- **Batch size**: 32.
- **Device**: GPU (NVIDIA T4).

3.3. Inference and Metrics

During validation and testing, we compute the raw logits z, convert to probabilities $p = \sigma(z)$, and binarize at threshold $t = 0.5$. We record:

- **AUROC**: area under the full ROC curve.
- **Balanced accuracy**: average of sensitivity and specificity.
- **Recall**: The ratio between the number of Positive samples correctly classified as Positive to the total number of Positive samples.
- **Macro F_1-score**: macro-averaged F1 score (harmonic mean of precision and recall per class), used due to the imbalanced dataset.
- **Confusion matrix**: to visualize true/false positives and negatives.

A schematic of the pipeline is shown in Figure 4.

4. Evaluation

4.1. Analysis of Baseline Performance

Loss Curve Analysis. As the previous baseline of phase 1, both the training and validation losses decrease steadily and remain closely aligned throughout all 20 epochs (figure 2), with no widening gap indicative of overfitting. Moreover, there is no clear trend toward a plateau in the validation loss, suggesting that the model has not yet reached its capacity for improvement. Consequently, our current run is too short both to identify an optimal stopping point and to observe diminishing returns. Note that all threshold-dependent metrics were calculated using Youden's point.

Ranking Metrics.
- **AUROC**: 0.909, up from 0.88 at baseline.
- **Macro-F_1 Score**: 0.778, exceeding the 0.72 baseline.
- **Balanced Accuracy**: 0.755, improving on the 0.71 baseline.
- **Recall**: 0.56 (not calculated in Phase 1 of the project).
- **Confusion Matrix** confirms the results obtained from the other metrics (Figure 3).

Grad-CAM visualizations (Figure 6) were employed to qualitatively assess the model's predictions. Although at first glance the model appears to focus on lesion areas in some cases (Figure 5), further inspection across multiple images revealed that, even when predictions are correct, the model sometimes attends to image corners rather than the lesions themselves. The underlying cause of this behavior remains unclear, and further investigation is needed to identify and mitigate any spurious cues the network may be exploiting.

Conclusion. We conclude that the new baseline outperforms the previous one: its improved metrics likely stem from applying weighted sampling to address the dataset's pronounced benign-class imbalance. As expected, since in the first milestone we did not implement any sampling, which resulted in considerable class imbalance.

4.2. Optimal Threshold Selection

To enhance classification performance beyond the default 0.5 cutoff, we computed Youden's J statistic,

$$J(t) = \text{TPR}(t) - \text{FPR}(t),$$

and used it to select the optimal decision threshold for our metrics, by maximizing J(t), we select the threshold that yields the largest sum of sensitivity and specificity, i.e. the point where the number of true positives and true negatives is jointly maximized.

4.3. Experiments

4.3.1. Baseline with Image Resizing to 300x300 15 epochs

This experiment yielded an AUROC of **0.906**, balanced accuracy of **0.727**, F1-score of **0.753**, and recall of **0.502**. Despite the reasonable metrics, this approach underperformed compared to the baseline. We believe the model may have required more training time to effectively learn the patterns, suggesting that increasing the number of epochs could improve performance.

4.3.2. Baseline with Mixup 0.2 (15 Epochs)

This experiment aimed to address class imbalance by applying mixup with a factor of 0.2. It achieved an AUROC of **0.884**, balanced accuracy of **0.674**, F1-score of **0.701**, and recall of **0.397**. Performance was lower than the baseline. MixUp "blends" every pair of images, which often requires more epochs for the network to unlearn those artificial hybrids and settle on clean class boundaries. Fifteen epochs may simply not have been enough for MixUp to pay off.

4.3.3. Baseline with Shades of Grey Preprocessing (15 Epochs)

This experiment introduced grayscale transformations to enhance model robustness by reducing reliance on color features. It produced an AUROC of **0.874**, balanced accuracy of **0.697**, F1-score of **0.725**, and recall of **0.443**. The results were lower than the baseline, indicating that this transformation did not improve performance in this case. This may be due to the reduced color information making the task more difficult, requiring a stronger model or longer training to compensate.

5. Conclusion

In this project, we used convolutional neural networks to identify cancerous lesions in dermoscopic images. Limited computational resources and a relatively small number of training epochs constrained our experiments, resulting in modest performance gains. Nonetheless, we achieved a solid AUROC of 0.909. Grad-CAM visualizations (Figure 6) reveal that, even when predictions are correct, the model sometimes attends to irrelevant corners of the image rather than the lesion itself. The cause of this behavior remains undetermined. Therefore, given these limitations, this model should not be used for real medical diagnoses.

6. Future Work

Building on our current baseline, future efforts will focus on:

- Expanding to a larger dataset. Due to GPU budget constraints, we did not utilize ISIC-2019; incorporating that dataset would be highly beneficial.
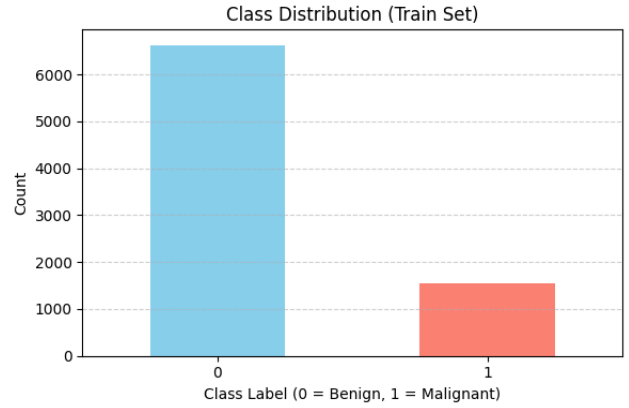

Figure 1. Class distribution in train, validation and test splits (81 % benign, 19 % malignant).
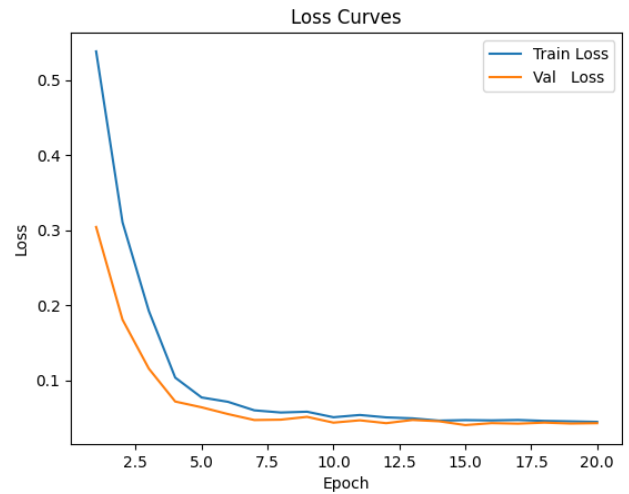

Figure 2. Training and validation loss across 20 epochs; curves overlap, showing stable learning but room for more training.

- Implementing 5-fold patient-level cross-validation to improve the generalizability of our results.
- Reconsidering layer freezing. Since EfficientNet was pretrained on ImageNet (natural images), freezing its early layers may hinder learning domain-specific features. Future experiments should investigate full fine-tuning from the start.
- Exploring more powerful architectures. For example, training a ConvNeXt model could further enhance performance given its proven effectiveness on similar image-classification tasks.
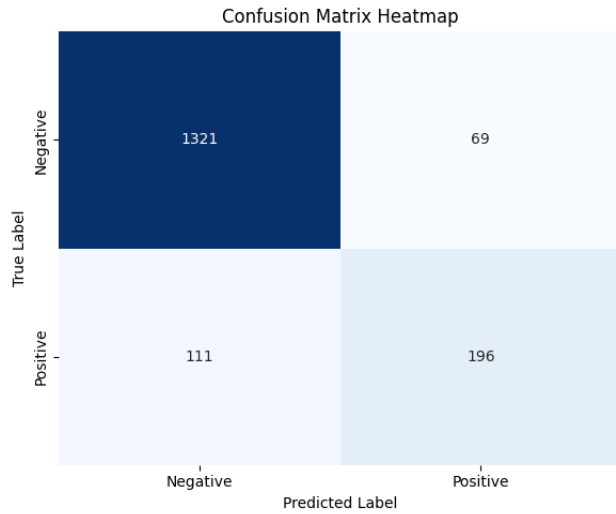
Figure 3. Confusion matrix at Youden-optimised threshold: TPs/TNs vs. FPs/FNs for malignant vs. benign lesions.
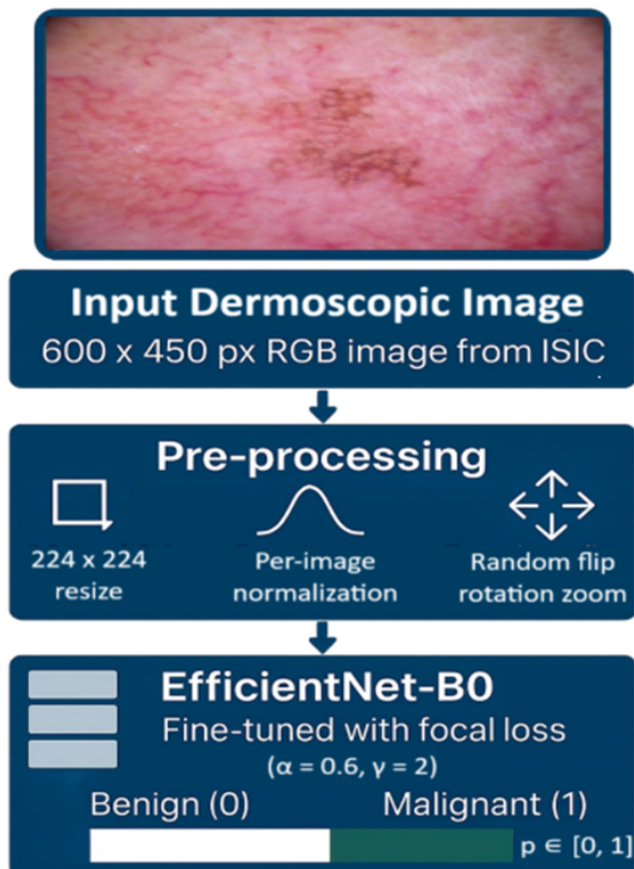

Figure 5. Grad-CAM heat-maps: top row correct predictions, bottom row incorrect; red areas show model attention.

Figure 4. End-to-end pipeline: ISIC download → preprocessing/augmentation → EfficientNet-B0 inference → metric reporting.

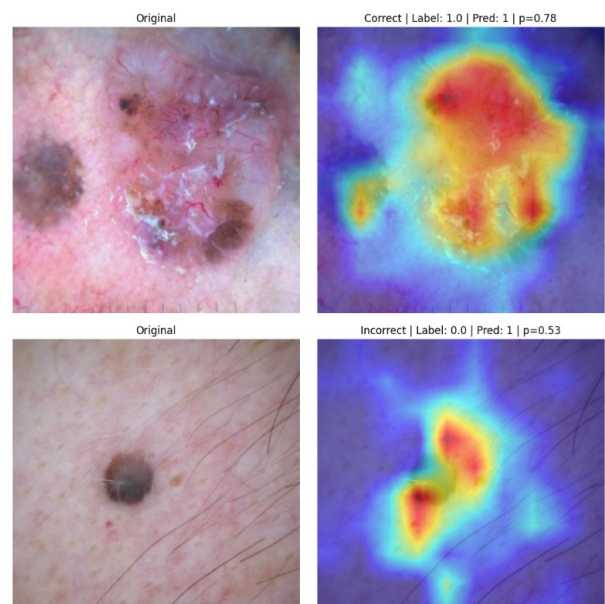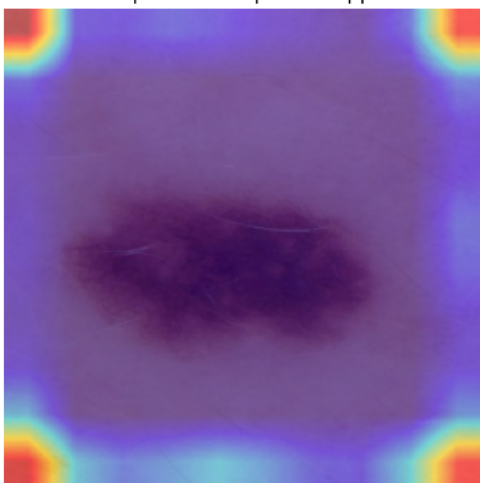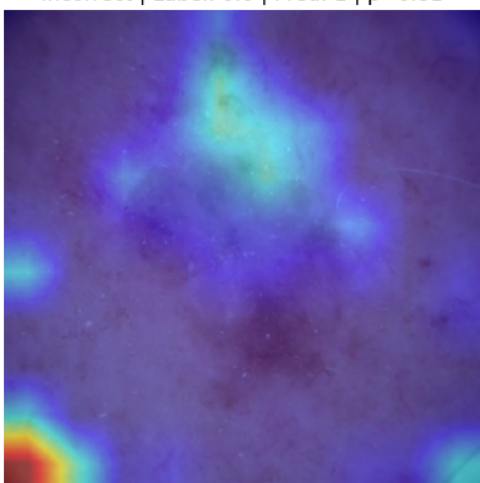Figure 6. Example misleading predictions: model focuses on background artefacts (bottom).